Energies **2015**, *8*, 12304-12313; doi:10.3390/en81012304

OPEN ACCESS

energies

ISSN 1996-1073

www.mdpi.com/journal/energies

Article

Effects of CO_2 Bubble Size, CO_2 Flow Rate and Calcium Source on the Size and Specific Surface Area of $CaCO_3$ Particles

Jun-Hwan Bang, Kyungsun Song, Sangwon Park, Chi Wan Jeon, Seung-Woo Lee and Wonbaek Kim *

Korea Institute of Geoscience and Mineral Resources, 124 Gwahak-ro, Yuseong-gu, Daejeon 305350, Korea; E-Mails: jhbang@kigam.re.kr (J.-H.B.); kssong@kigam.re.kr (K.S.); psw1231@kigam.re.kr (S.P.); jcw@kigam.re.kr (C.W.J.); swlee21th@kigam.re.kr (S.-W.L.)

* Author to whom correspondence should be addressed; E-Mail: wbkim@kigam.re.kr; Tel.: +82-42-868-3659.

Academic Editor: Vijay Kumar Thakur

Received: 18 August 2015 / Accepted: 19 October 2015 / Published: 27 October 2015

Abstract: The effects of CO_2 flow rate and calcium source on the particle size (PS) and specific surface area (SSA) of $CaCO_3$ particles were evaluated using microbubble generator (MBG) and air diffuser (AD) systems. The carbonate mineralization (CM) and precipitated calcium carbonate (PCC) methods were employed to produce $CaCO_3$ using gypsum and $Ca(OH)_2$ as the calcium sources, respectively. The $CaCO_3$ particles prepared using the MBG were smaller (with larger specific surface area) than those obtained using the conventional AD, regardless of the calcium source. The average PSs were 2–3 and 7–9 μm for the MBG and AD systems, respectively. Moreover, the PS and SSA of the particles prepared using the MBG were not greatly affected by the CO_2 injection rate. This study clearly demonstrates that the use of an MBG ensures the stable production of fine $CaCO_3$ particles using various calcium sources and a wider range of CO_2 flow rates.

Keywords: carbonate mineralization; CO_2 fixation; $CaCO_3$; particle size; specific surface area; microbubble

1. Introduction

Microbubbles (MBs) are very tiny bubbles in liquids, with diameters of several tens of micrometers [1]. One typical use of MBs is water purification, achieved by increasing the dissolved oxygen concentration in polluted water. As an extension of the use of MBs to a wider range of applications, the recovery of fine particles [2] and the precipitation of $CaCO_3$ using $Ca(OH)_2$ [3] have been reported. This application is apparently related to a physical property of the MBs not found in ordinary bubbles in liquids, namely that the concentration of a specific gas in a liquid remains higher for longer if the gas is contained in MBs.

Equation (1) explains the stability of the size of MBs:

$$\sigma = \left(\frac{\partial G}{\partial A}\right)_{T,P} \tag{1}$$

where, σ, *G*, and *A* are the surface tension, Gibbs free energy, and surface area, respectively, of a CO_2 bubble:

$$J_{\mathrm{CO_2}z} = -D_{\mathrm{CO_2}A}\frac{dC_{\mathrm{CO_2}}}{d_z} \tag{2}$$

where, $J_{\mathrm{CO_2}z}$ is the concentration rate of CO_2 diffused in the *z* direction (mol/m^2·s), $D_{\mathrm{CO_2}A}$ is the diffusion coefficient of CO_2 through the suspension (m^2/s), $dC_{\mathrm{CO_2}}$ is the CO_2 concentration difference (mol/m^3), and d_z is the length difference in the *z* direction (m).

The surface tension (σ) increases as the surface area (*A*) of the bubble decreases, if the energy (*G*) in the two states is identical. Additionally, decreasing the surface area means decreasing the volume and floatation rate of the bubble. Therefore, MBs can remain suspended for longer than ordinary bubbles. The increased concentration of a gas in an aqueous phase enhances the diffusion rate. Fick's first law of diffusion, presented in Equation (2), shows that the diffusion rate of CO_2 is enhanced in the *z* direction, if the concentration of CO_2 increases. The impact of these qualities of MBs in increasing the concentration of a gas is different from that of ordinary bubbles (as is evident on breathing into water through a straw). We have reported that a microbubble generator (MBG) precipitated smaller calcium carbonate particles faster than an ordinary air diffuser with 3 cm diameter did [3]. Feng *et al.* [4] also obtained smaller $CaCO_3$ particles by reducing the frit pore size used for CO_2 bubbling in a $Ca(OH)_2$ suspension: The carbonate mineralization (CM) method is used to fix CO_2 as a carbonate mineral (*i.e.*, $CaCO_3$). With this method, carbonates are formed as precipitates from the chemical reaction between CO_2 and alkali earth metals such as calcium [5–7]. This method originated from a process for producing precipitated $CaCO_3$ [8]. Although this chemical reaction is simple and well known, as pointed out by Haywood *et al.* [9], some consideration of the reaction rate and efficiency of metal extraction is needed to realize a successful CO_2 fixation method. $Ca(OH)_2$ or CaO (the dehydrated form of $Ca(OH)_2$) is the calcined form of $CaCO_3$ (formed by dissociation of CO_2 when heated above 900 K). Therefore, for the purpose of CO_2 fixation, $Ca(OH)_2$ is not a good choice as a calcium source. Naturally obtainable gypsum is a better calcium-supply material for CM than $Ca(OH)_2$ because gypsum does not emit CO_2 as it does not involve thermal decomposition. Previously, we examined CM using $CaSO_4 \cdot 2H_2O$ (gypsum) as the calcium source with a NaOH solution, and using CO_2 MBs. Our results confirmed the enhanced efficiency of the reaction with this calcium source [10]. The crystal phases of gypsum, calcite, and portlandite were affected by the experimental conditions, such as differences in the concentration ratio of OH^{-} to Ca^{2+}. Herein, the particle size (PS) and specific surface area (SSA) of $CaCO_3$ (calcite) produced by CM from gypsum are compared with those of particles precipitated using the precipitated calcium carbonate (PCC) method with $Ca(OH)_2$ as the calcium source. Additionally, the effect of CO_2 bubble size of larger bubbles from an air diffuser (AD) and tiny bubbles from MBG on the PS and SSA was estimated by the results from the experiments and the reference [4]. The PS and SSA results presented here for the PCC method are from our previous research [11]. The results from the current study should be useful for designing a CM process to achieve two aims: effective CO_2 fixation, and production of $CaCO_3$ with properties useful for industrial use.

2. Materials and Methods

2.1. Raw Materials

Gypsum (96%, Junsei Chemicals, Tokyo, Japan) was selected as the calcium source for CM (concentration of 0.3 M). NaOH (97%, Samchun Chemicals, Seoul, Korea) was dissolved in water to prepare a 6 M stock solution, 100 mL of which was added to the gypsum suspension. Microbubbles of 99.9% CO_2 were injected from an MBG (at 0.4, 0.8 and 1.0 L/min) into the 1 L of NaOH-dosed gypsum suspension. A schematic of the MBG process was previously published [10]. All experiments were repeated at least twice.

For the PCC method, $Ca(OH)_2$ (96%, concentration 0.3 M, Junsei Chemicals) was selected as the calcium source of $CaCO_3$ precipitate. The CO_2 MBs were injected into the 1 L of the suspension at the same flow rates used for the CM method. A detailed experimental scheme for this can be found in another report [3].

Table 1 shows the specifications of the calcium supply materials, and Figure 1 indicates the 70,000× SEM images of the raw materials. All the solutions and suspensions were prepared using deionized water (Milli-Q Advantage A10, Millipore, Billerica, MA, USA).

Table 1. Specifications, particle size (PS), and specific surface area (SSA) of the raw materials.

Reagent	Assay (%)	PS (μm)	SSA (m^2/g)	Concentration (M)	Volume (L)
Gypsum	96	42.9	9.9	0.3	1
$Ca(OH)_2$	96	8 *	-	0.3	1

* The PS results for $Ca(OH)_2$ are from our previous paper [11].

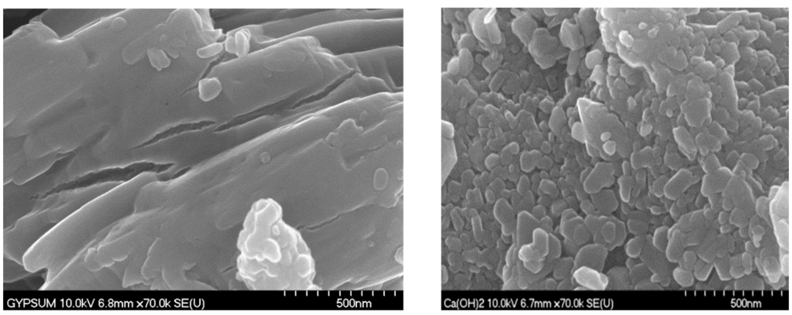

(**a**) (**b**)

Figure 1. SEM images of the calcium source materials: (**a**) Gypsum and (**b**) $Ca(OH)_2$.

2.2. Characterization

Circulation of the suspension, and injection of CO_2, were stopped when the pH (measured every 30 s, Orion 3 Star, Thermo Scientific, Waltham, MA, USA) of the suspension did not vary, and was ~7–8. The particles were collected using a nylon membrane (0.2 μm pore size, Whatman, Brentford, UK), dried at 303 K for at least 48 h; then, the PS was measured (Mastersize 2000, Malvern Instruments, Malvern, UK). The SSA was measured using Tristar 3000 (Micromeritics, Norcross, GA, USA) and Quadrasorb SI 4S (Quantachrome Instruments, Boynton Beach, FL, USA) analyzers after pre-treatment at 523 K to remove all moisture from the pores. The nitrogen gas provided was assumed to be adsorbed in multiple layers on the surfaces of $CaCO_3$ particles. The images of the particles were obtained using a Field Emission Scanning Electron Microscope (FE-SEM) (S4700, Hitachi, Japan) located at Korea Basic Science Institute (KBSI) Jeonju Center. The PS and SSA of the particles presented here for the PCC method were from previous research [11].

2.3. Control Experiments

A conventionally used ceramic air diffuser (AD) was employed to inject CO_2 into the gypsum and $Ca(OH)_2$ suspension to compare the effect of CO_2 MB on the characteristics of $CaCO_3$ particles produced by both methods: CM and PCC. A 3-cm diameter AD designed for use in a fishbowl was placed in a 2000-mL beaker. A 0.3 M gypsum suspension was used as calcium supplement. For the MBG experiments, 100 mL of 6 M NaOH solution was added to the 1 L of gypsum suspension, and the CO_2 flow rate was 0.8 L/min. Magnetic stirring at 300 rpm was used to compensate for the weak mixing of the suspensions compared with that during the MBG process.

3. Results and Discussion

The average particle size of the raw gypsum was 42.9 μm (Table 1). The initial pH of the gypsum suspension without NaOH solution was around 8.5. While the gypsum suspension circulated with CO_2 MBs at 0.8 L/min through the MBG, the pH of the suspension decreased to ~7 and remained stable from the 4th minute of the process. After 16 min of circulation, the size of the gypsum particles was 25 μm. This reduction in size was not introduced by CM because NaOH was not added to the gypsum suspension; this was not a favorable condition for production of carbonate ions. The reduction in PS was due to frequent and random collisions between the suspended particles, CO_2 MBs, and parts of the MBG, owing to the turbulent flow resulting from the high flow rate [12]. The much smaller calcium-supply particles created by the MBs had much greater surface area and increased the reaction rates of both methods (CM and PCC). Ramachandran and Sharma [13] showed that, in theory, smaller particles should enhance chemical reactions between gas and liquid phases.

After 100 mL of NaOH solution was added, the gypsum suspension and CO_2 MBs were circulated through the MBG. The particles were collected when the suspension was around pH 7 and steady (after about 13 min circulation). XRD analysis revealed that all the collected particles were calcite [10]. The particle sizes obtained by CM with gypsum suspension were 2.4, 2.6 and 2.9 μm (black squares (□) in Figure 2), when the CO_2 injection rates were 0.4, 0.8 and 1.0 L/min, respectively. The average PS was 2.6 μm with a standard deviation of 0.3 μm.

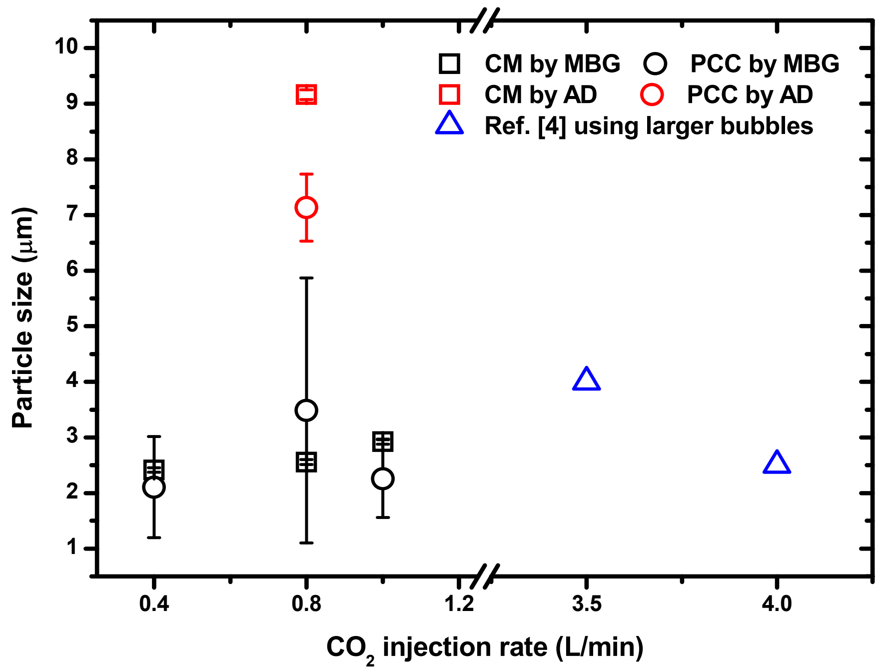

Figure 2. Particle size (PS) of $CaCO_3$ produced by carbonate mineralization (CM) and precipitated calcium carbonate (PCC) from gypsum (squares □) and $Ca(OH)_2$ (circles ○). The effect of CO_2 injection methods (microbubble generator (MBG) and air diffuser (AD)) on the PS were marked additionally in black and red, respectively. The horizontal axis indicates the CO_2 injection rate into the calcium-source suspensions. The PS results using $Ca(OH)_2$ are from our previous paper [11]. The values in blue triangles are from reference [4] when 101–160 μm bubbles were used, and these are approximate values. The standard deviation was obtained from the repeated experimental results at least twice.

For comparison, the size of the particles obtained by PCC with a suspension of $Ca(OH)_2$ were 2.1, 3.5 and 2.3 μm (black circles (○) in Figure 2) when the CO_2 injection rates were 0.4, 0.8 and 1.0 L/min, respectively. The average PS was 2.6 ± 0.8 μm [11]. It is interesting that the size of the $CaCO_3$ particles was almost the same regardless of the type of calcium source, when the MBG was used for either the CM or the PCC method.

However, the PS was not the same when an AD was used to inject CO_2 into the calcium-source suspension, for CM (9.2 ± 0.1 μm) or PCC (7.1 ± 0.6 μm) (red marks in Figure 2). Much smaller $CaCO_3$ particles were produced using the MBG than with the AD, regardless of the calcium source. Under the same CO_2 injection rate of 0.8 L/min into the calcium source suspension, tiny CO_2 bubbles by MBG produced the calcite particles sized in from 2.6 to 3.5 μm, and larger CO_2 bubbles by AD did the calcite particles sized in from 7.1 to 9.2 μm. MBG makes the CO_2 concentration higher even when the flow rate of CO_2 into the calcium-source suspension was low. For this reason, supersaturation of carbonate ions can be induced in the suspension, which will precipitate smaller $CaCO_3$ particles because of the higher nucleation rate [14]. It was observed that the PS of $CaCO_3$ was not sensitive to the CO_2 flow rate when a MBG was used. In contrast, when an AD or a gas distributor was used, the PS was significantly affected by the gas flow rate. Feng *et al.* [4] investigated the effect of CO_2 flow rate and bubble size on the PS of $CaCO_3$. A flow rate increment from 3.5 to 4 L/min, reduced the PS from 4 to 2.5 μm. For comparison, their results are also included as blue triangles (Δ) in Figure 2.

Figure 3 shows SEM images of Figure 3a raw gypsum and Figure 3b gypsum circulated through the MBG for 16 min without a dose of NaOH. Evidently, the gypsum particles become significantly smaller during circulation. Therefore, the SSA of the particles was expected to increase owing to this refinement. The raw gypsum crystals were covered by numerous fine particles (Figure 3a), which greatly increased the surface area. Therefore, the surface area would be decreased if these surface particles were dissolved during circulation. The very flat surface of gypsum after circulation (Figure 3b) supports this explanation. The expected increase in the measured SSA was not observed. Instead, the SSA of the gypsum decreased from 9.9 to 6.1 m^2/g during circulation, despite significant reduction in the PS. The reason for this discrepancy can be observed in the SEM images. The high flow rate provided by the MBG is expected to readily dissolve these tiny particles on the surface of gypsum crystals.

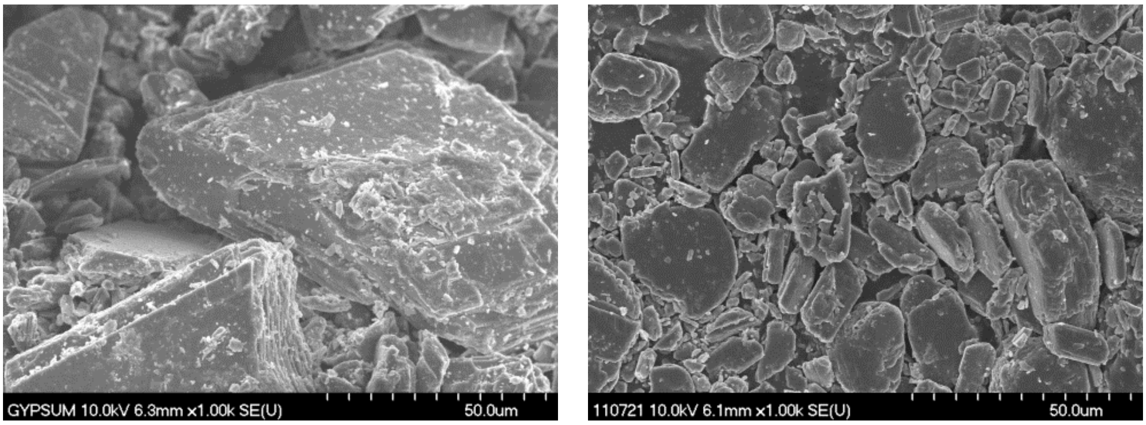

(**a**) (**b**)

Figure 3. Scanning Electron Microscope (SEM) images of gypsum: (**a**) Raw gypsum with tiny particles (<2 μm) on the surface of larger particles; (**b**) Gypsum after circulation for 16 min through the MBG: The tiny particles disappeared and the large particles were broken into smaller ones.

The SSAs of the $CaCO_3$ particles prepared by CM or PCC with CO_2 MBs were similar whether the calcium source was $Ca(OH)_2$ or gypsum. Figure 4 shows the effect of the CO_2 injection rate on the SSA for both the MBG and AD. The SSA of the particles from the gypsum suspension after the MBG process (black squares (□) in Figure 4) was 23.7, 22.0 and 17.5 m^2/g at the CO_2 rates of 0.4, 0.8 and 1.0 L/min, respectively. The average value was 21.1 ± 3.20 m^2/g: the standard deviation of 15% being rather high. In comparison, the SSA of particles produced by PCC with $Ca(OH)_2$ was 21.7, 22.2 and 22.4 m^2/g at CO_2 rates of 0.4, 0.8 and 1.0 L/min, respectively (black circles (○) in Figure 4), with an average SSA of 22.1 ± 0.36 m^2/g [11]. This result agrees with the PS data in the sense that the SSA values are almost constant when using the MBG, regardless of the calcium source. The SSA of particles prepared at a CO_2 flow rate of 0.8 L/min, using the AD (red marks in Figure 4), were significantly less than for those obtained using the MBG. In this case, the particles prepared by CM with gypsum had a SSA of 10.7 ± 3.3 m^2/g, whereas those prepared with $Ca(OH)_2$ had a SSA of 17.2 ± 6.1 m^2/g as AD supplied larger CO_2 into the calcium source suspension; MBG with tiny CO_2 bubbles produce the calcite particles with larger SSA (22.0–22.2 m^2/g).

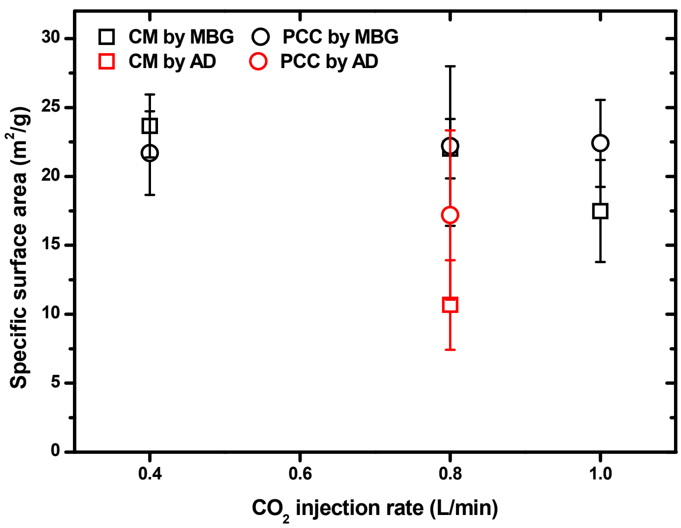

Figure 4. SSA of $CaCO_3$ produced by CM and PCC from gypsum (squares □) and $Ca(OH)_2$ (circles ○) respectively. The effect of the CO_2 injection methods (MBG and AD) on the SSA were marked in black and red, respectively. The horizontal axis indicates the CO_2 injection rate into the calcium-source suspensions. The SSA results using $Ca(OH)_2$ are from our previous paper [11]. The standard deviation was obtained from the repeated experimental results at least twice.

Figure 5 shows SEM images of the $CaCO_3$ particles obtained from the CM process (gypsum source) and PCC process ($Ca(OH)_2$ source) using either MBG or AD. The particles prepared using the MBG appear smaller than those prepared using AD, regardless of calcium source. In addition, the particles produced using the MBG had a narrower size distribution (Figure 5a,b), than those using AD (Figure 5c,d). This was probably because of comparatively larger clusters in the latter. The SSA is affected by the size of primary particles that are agglomerate to form larger (secondary) particles. The size of primary particles can be calculated by Equation (3) when the particles are granular [15]. Table 2 shows the results for primary particle size calculated using this equation. These values were in accordance with the SEM images in Figure 5 when the MBG was used. However, the PS of the primary $CaCO_3$ particles produced using the AD were not matched with the SEM results in Figure 5 due to the irregular shapes of the particles and their agglomerates. In this case, the contacted surfaces between the irregular shaped primary particles were larger than the granular particles in order to the SSA would be reduced:

$$d = 6/(S_g \cdot \rho_g) \tag{3}$$

where, d is primary particle size, S_g is SSA, and ρ_g is density of the particles (in this case 2.71 g/cm^3 for calcite of $CaCO_3$).

The novelty of this study is that the size of the $CaCO_3$ particles prepared using the MBG were finer and almost identical in size (~2.6 μm and 22 m^2/g) regardless of the calcium source, whereas the use of an AD produced coarser $CaCO_3$ particles (~8 μm and less than 17 m^2/g). Generally, when such $CaCO_3$ particles are used in paper making, it is said that their finer PS and greater SSA enhance smoothness and printing quality. A rationale for the homogeneities in (primary) PS and SSA may be that the MBG causes changes in the fluid dynamics, such as the surface tension and buoyancy of bubbles in the calcium-source suspension, which are quite different from those obtained with the AD.

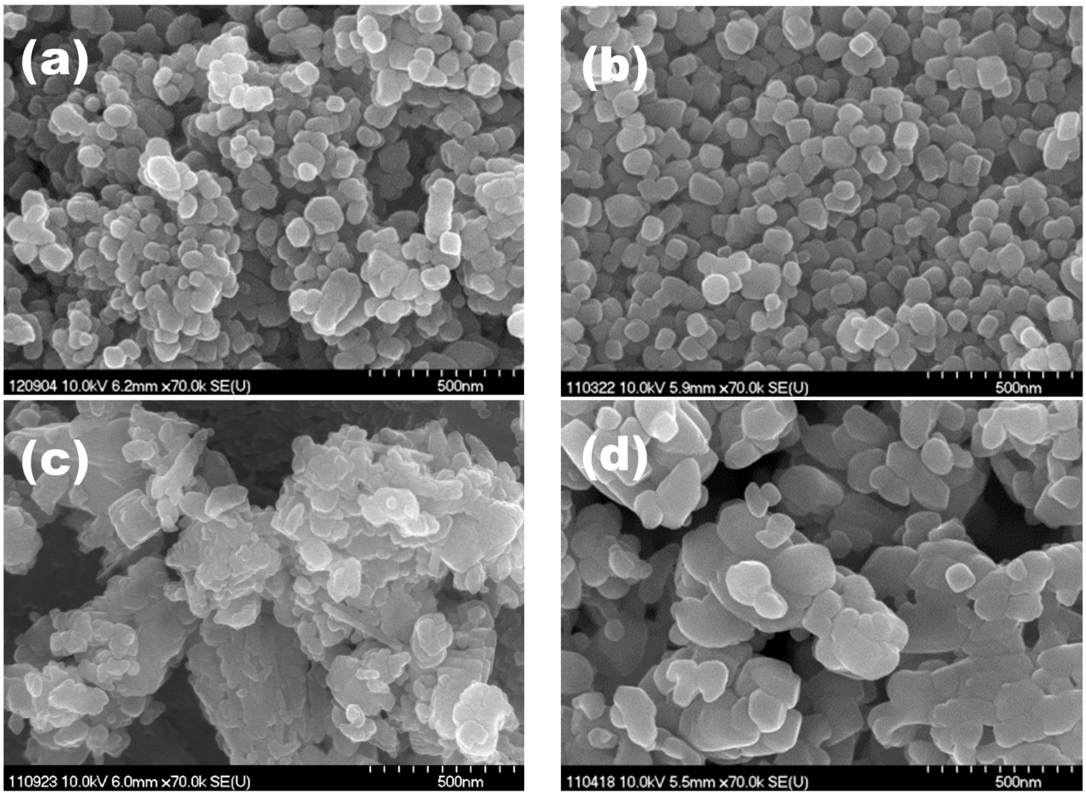

Figure 5. SEM images of $CaCO_3$ produced by AD and MBG using gypsum and $Ca(OH)_2$: (**a**) gypsum by MBG; (**b**) $Ca(OH)_2$ by MBG; (**c**) gypsum by AD and (**d**) $Ca(OH)_2$ by AD. The particles in this panel were obtained CO_2 flow at 0.8 L/min, with AD and MBG.

Table 2. Calculated size of the primary particles based on specific surface area.

CO_2 Rate (L/min)	Size of the Primary Particles (nm)			
	CM by MBG	PCC by MBG	CM by AD	PCC by AD
0.4	94	102	-	-
0.8	101	100	207	129
1.0	127	99	-	-

According to Henry's law, the degree of solubility of a gas in aqueous media depends on the pressure and temperature. The addition of chemicals such as amines [16–18] and ammonia [19–21] could enhance the solubility of CO_2 by forming complexes. Moreover, changes in the physical properties of a gas bubble, such as decreasing the bubble size, could also increase their solubility under given conditions of atmospheric pressure and temperature [3,10,22]. The strong surface tension of MBs described in Equation (1) causes these results. This will improve the ability to build rather small, unpressurized CM facilities, to use less and thus reduce the cost of CO_2 sorbent chemicals, and to reduce the loss of whiteness of $CaCO_3$ particles due to those chemicals. The use of the MBG accelerates the nucleation rate of $CaCO_3$ due to the enhanced diffusion rate indicated in Equation (2), which decreases the PS. In addition, Gibbs-Thomson and Ostwald ripening effects exert an influence on the PS, with a limit for $CaCO_3$ near 2 μm [23]. This appears to agree with our result of PS around 2 μm, regardless of the calcium source, and of the process (CM or PCC), when the MBG was used.

4. Conclusions

The effect of the MBG on the PS and SSA of $CaCO_3$ particles prepared using the CM process from gypsum was evaluated. The properties of the particles obtained by the PCC process from $Ca(OH)_2$ were compared. The PS and SSA were almost identical regardless of calcium source, and CO_2 flow rates if MBG used. Moreover, the particles produced by MBG had smaller size (around 2 μm) and greater SSA (around 22 m^2/g) than those obtained in the control experiments by AD (around 8 μm and less than 17 m^2/g). This result was caused by innate qualities of the MBs: strong surface tension and enhanced diffusion rate. The results from this study are expected to help predict the qualities of the particles produced by CM from various calcium sources using MBG.

Acknowledgments

This research was supported by the Basic Research Project (15-3418) of the Korea Institute of Geoscience and Mineral Resources (KIGAM), funded by the Ministry of Science, Information and Communication Technology (ICT) and Future Planning.

References

1. Parmar, R.; Majumder, S.K. Microbubble generation and microbubble-aided transport process intensification—A state-of-the-art report. *Chem. Eng. Process. Process Intensif.* **2013**, *64*, 79–97.
2. Liao, Y.; Liu, J.; Cao, Y.; Zhu, X. Operation diagnosis of an industrial flotation column at the Xuehu Coal preparation plant. *Int. J. Coal Prep. Util.* **2014**, *34*, 296–305.
3. Bang, J.-H.; Jang, Y.N.; Kim, W.; Song, K.S.; Jeon, C.W.; Chae, S.C.; Lee, S.-W.; Park, S.-J.; Lee, M.G. Precipitation of calcium carbonate by carbon dioxide microbubbles. *Chem. Eng. J.* **2011**, *174*, 413–420.
4. Feng, B.; Yong, A.K.; An, H. Effect of various factors on the particle size of calcium carbonate formed in a precipitation process. *Mater. Sci. Eng. A* **2007**, *445–446*, 170–179.
5. Oelkers, E.H.; Gislason, S.R.; Matter, J. Mineral Carbonation of CO_2. *Elements* **2008**, *4*, 333–337.
6. Bałdyga, J.; Henczka, M.; Sokolnicka, K. Utilization of carbon dioxide by chemically accelerated mineral carbonation. *Mater. Lett.* **2010**, *64*, 702–704.
7. Chen, Z.-Y.; O'Connor, W.K.; Gerdemann, S.J. Chemistry of aqueous mineral carbonation for carbon sequestration and explanation of experimental results. *Environ. Prog.* **2006**, *25*, 161–166.
8. Teir, S.; Eloneva, S.; Zevenhoven, R. Production of precipitated calcium carbonate from calcium silicates and carbon dioxide. *Energy Convers. Manag.* **2005**, *46*, 2954–2979.
9. Haywood, H.; Eyre, J.; Scholes, H. Carbon dioxide sequestration as stable carbonate minerals—Environmental barriers. *Environ. Geol.* **2001**, *41*, 11–16.
10. Bang, J.-H.; Kim, W.; Song, K.S.; Jeon, C.W.; Chae, S.C.; Cho, H.-J.; Jang, Y.N.; Park, S.-J. Effect of experimental parameters on the carbonate mineralization with $CaSO_4 \cdot 2H_2O$ using CO_2 microbubbles. *Chem. Eng. J.* **2014**, *244*, 282–287.
11. Bang, J.-H.; Jang, Y.N.; Kim, W.; Song, K.S.; Jeon, C.W.; Chae, S.C.; Lee, S.-W.; Park, S.-J.; Lee, M.G. Specific surface area and particle size of calcium carbonate precipitated by carbon dioxide microbubbles. *Chem. Eng. J.* **2012**, *198–199*, 254–260.

12. Yagi, H.; Nagashima, S.; Hikita, H. Semibatch precipitation accompanying gas-liquid reaction. *Chem. Eng. Commun.* **1988**, *65*, 109–119.
13. Ramachandran, P.A.; Sharma, M.M. Absorption with fast reaction in a slurry containing sparingly soluble fine particles. *Chem. Eng. Sci.* **1969**, *24*, 1681–1686.
14. Jones, A.G.; Hostomsky, J.; Zhou, L. On the effect of liquid mixing rate on primary crystal size during the gas-liquid precipitation of calcium carbonate. *Chem. Eng. Sci.* **1992**, *47*, 3817–3824.
15. Yang, J.-H.; Shih, S.-M. Preparation of high surface area $CaCO_3$ by bubbling CO_2 in aqueous suspensions of $Ca(OH)_2$: Effects of $(NaPO_3)_6$, $Na_5P_3O_{10}$, and Na_3PO_4 additives. *Powder Technol.* **2010**, *197*, 230–234.
16. Chen, Y.-H.; Lu, D.-L. Amine modification on kaolinites to enhance CO_2 adsorption. *J. Colloid Interface Sci.* **2014**, *436*, 47–51.
17. Chen, C.; Kim, J.; Ahn, W.-S. CO_2 capture by amine-functionalized nanoporous materials: A review. *Korean J. Chem. Eng.* **2014**, *31*, 1919–1934.
18. Gomes, J.; Santos, S.; Bordado, J. Choosing amine-based absorbents for CO_2 capture. *Environ. Technol.* **2015**, *36*, 19–25.
19. Jo, H.; Park, S.-H.; Jang, Y.-N.; Chae, S.-C.; Lee, P.-K.; Jo, H.Y. Metal extraction and indirect mineral carbonation of waste cement material using ammonium salt solutions. *Chem. Eng. J.* **2014**, *254*, 313–323.
20. Dri, M.; Sanna, A.; Maroto-Valer, M.M. Dissolution of steel slag and recycled concrete aggregate in ammonium bisulphate for CO_2 mineral carbonation. *Fuel Process. Technol.* **2013**, *113*, 114–122.
21. Wang, X.; Maroto-Valer, M.M. Integration of CO_2 Capture and Mineral Carbonation by Using Recyclable Ammonium Salts. *ChemSusChem* **2011**, *4*, 1291–1300.
22. Jung, S.; Dodbiba, G.; Fujita, T. Mineral carbonation by blowing incineration gas containing CO_2 into the solution of fly ash and ammonia for ex situ carbon capture and storage. *Geosyst. Eng.* **2014**, *17*, 125–135.
23. Mullin, J.W. *Crystallization*, 3rd ed.; Butterworth-Heinemann Ltd.: Oxford, UK, 1993; p. 237.